

# Atomic Force Microscopy Studies of Ganglioside GM1 Domains in Phosphatidylcholine and Phosphatidylcholine/Cholesterol Bilayers

Chunbo Yuan and Linda J. Johnston

Stearie Institute for Molecular Sciences, National Research Council Canada, Ottawa, ON K1A 0R6 Canada

**ABSTRACT** The distribution of ganglioside in supported lipid bilayers has been studied by atomic force microscopy. Hybrid dipalmitoylphosphatidylcholine (DPPC)/dipalmitoylphosphatidylethanolamine (DPPE) and (2:1 DPPC/cholesterol)/DPPE bilayers were prepared using the Langmuir Blodgett technique. Egg PC and DPPC bilayers were prepared by vesicle fusion. Addition of ganglioside GM1 to each of the lipid bilayers resulted in the formation of heterogeneous surfaces that had numerous small raised domains (30–200 nm in diameter). Incubation of these bilayers with cholera toxin B subunit resulted in the detection of small protein aggregates, indicating specific binding of the protein to the GM1-rich microdomains. Similar results were obtained for DPPC, DPPC/cholesterol, and egg PC, demonstrating that the overall bilayer morphology was not dependent on the method of bilayer preparation or the fluidity of the lipid mixture. However, bilayers produced by vesicle fusion provided evidence for asymmetrically distributed GM1 domains that probably reflect the presence of ganglioside in both inner and outer monolayers of the initial vesicle. The results are discussed in relation to recent inconsistencies in the estimation of sizes of lipid rafts in model and natural membranes. It is hypothesized that small ganglioside-rich microdomains may exist within larger ordered domains in both natural and model membranes.

## INTRODUCTION

Despite the traditional view of a lipid bilayer as a dynamic, fluid environment, there is increasing evidence that organization of lipids and other membrane components into domains plays a crucial role in many cellular functions. Much of the evidence for the existence of lipid domains comes from indirect experiments such as the isolation of detergent-insoluble membrane fractions that are rich in cholesterol, saturated lipids and some glycolipids, and membrane-anchored proteins (Brown and London, 1997, 1998; Brown and Rose, 1992). Coexistence of liquid-ordered and liquid-disordered phases has been observed for lipid mixtures that are similar in composition to detergent-resistant membranes (Ahmed et al., 1997; Schroeder et al., 1995). This has led to a model of lipid rafts wherein preferential packing of sphingolipids and cholesterol is mediated by hydrogen bonding and leads to lipid microdomains or rafts that are in the liquid-ordered phase (Brown and London, 2000; Simons and Ikonen, 1997, 2000). These domains are believed to play a role in signal transduction and membrane trafficking. Other support for the formation of lipid rafts comes from experiments where labeled antibodies or particles are used to visualize the domains (Jacobson and Dietrich, 1999). For example, a recent energy transfer experiment demonstrates that a GPI-anchored protein, the folate receptor, is clustered into domains that are 70 nm or smaller in cells (Varma and Mayor, 1998). Similarly, measurement of the local diffusion

of membrane-associated proteins leads to estimates of  $26 \pm 13$  nm for the size of rafts in fibroblasts (Pralle et al., 2000).

Supported phospholipid monolayers and bilayers have been extensively studied as membrane models and have provided a wealth of information on lipid properties and organization (Sackmann, 1996). The lateral mobility of lipids in supported bilayers makes them particularly useful models because they retain much of the fluidity associated with actual cellular membranes (Boxer, 2000). Recently, atomic force microscopy (AFM) and related techniques have been shown to be ideally suited for obtaining detailed morphological information on phase separation for supported lipid monolayers and bilayers (Bassereau and Pincet, 1997; Chi et al., 1993; Dufrene et al., 1997; McKiernan et al., 2000; Mou et al., 1995; Reviakine and Brisson, 2000; Reviakine et al., 2000; Schneider et al., 2000; Sparr et al., 1999; Vie et al., 1998; Yuan and Johnston, 2000). Of particular relevance to the question of lipid microdomains are recent AFM experiments that have shown that ganglioside GM1, a commonly used raft marker, is localized in small sub-micron-sized domains in various phosphatidylcholine (PC) monolayers as well as in L- $\alpha$ -dipalmitoylphosphatidylcholine (DPPC)/cholesterol monolayers deposited on mica by Langmuir-Blodgett transfer (Vie et al., 1998; Yuan and Johnston, 2000). Although clustering of GM1 in model membranes has been suggested on the basis of earlier electron microscopy (Peters and Grant, 1984; Peters et al., 1984) and electron spin resonance (ESR) (Delmelle et al., 1980) results, data from other studies have indicated a random distribution of GM1 (Thompson et al., 1985).

Fluorescence microscopy of monolayers at the air-water interface has shown that GM1 is localized in relatively large domains of a condensed cholesterol/lipid complex-rich phase that is thought to be analogous to rafts in cell membranes (Radhakrishnan et al., 2000). Recent studies by flu-

Received for publication 19 March 2001 and in final form 9 May 2001.

Address reprint requests to Dr. Linda J. Johnston, Steacie Institute for Molecular Sciences, National Research Council Canada, Ottawa, ON K1A 0R6 Canada. Tel.: 613-990-0973; Fax: 613-952-0068; E-mail: Linda.Johnston@nrc.ca.

© 2001 by the Biophysical Society

0006-3495/01/08/1059/11 \$2.00

orescence microscopy on supported lipid bilayers and giant unilamellar vesicles composed of raft-like lipid mixtures provide evidence for micron-sized domains that are more ordered than the surrounding fluid phase and that are enriched in GM1 (Dietrich et al., 2001). These results provide some of the most direct evidence so far for the existence of a liquid-ordered raft-like phase that concentrates glycosphingolipids. However, the results are in contrast to observations in natural membranes where much smaller sub-micron-sized rafts have been postulated. It has been suggested that the difference may reflect the role of the cytoskeleton in regulating aggregation in cell membranes (Dietrich et al., 2001).

We have used AFM to study the distribution of ganglioside GM1 in supported lipid bilayers. The results described herein demonstrate that GM1 is heterogeneously distributed in small domains in PC and PC/cholesterol bilayers. The evidence for domain formation is provided both by the observation of small higher domains upon incorporation of ganglioside into bilayers and also by using cholera toxin binding to conclusively show the location of the ganglioside in the bilayer. Similar results have been obtained using either vesicle fusion or Langmuir-Blodgett transfer for bilayer preparation.

## MATERIALS AND METHODS

### Materials

DPPC, L- $\alpha$ -dimyristoylphosphatidylcholine (DMPC), L- $\alpha$ -dipalmitoylphosphatidylethanolamine (DPPE), and L- $\alpha$ -egg phosphatidylcholine (EPC) were obtained from Avanti Polar Lipids (Alabaster, AL). Monosialoganglioside-GM1 from bovine brain, cholesterol, and cholera toxin B (CTB) subunit were from Sigma Chemical Co. (St. Louis, MO). DPPC, EPC, and cholesterol were dissolved in chloroform at 1 mg/ml. GM1 and DPPE were dissolved in chloroform/methanol (v/v, 4:1) at 0.5 mg/ml and 1 mg/ml, respectively.

### Hybrid bilayers

The hybrid bilayers were prepared by the Langmuir-Blodgett technique. First, a DPPE monolayer was spread on a Langmuir-Blodgett trough (NIMA 611, Coventry, UK) using Milli-Q water as the subphase. After a 10-min evaporation of the solvent, the monolayer was compressed at 50 cm<sup>2</sup>/min to the required surface pressure. The surface pressure was measured with a precision of 0.1 mN/m using a Wilhelmy balance. The monolayer was annealed twice before transferring to freshly cleaved, hydrophilic mica at a surface pressure of 45 mN/m by vertical deposition at a dipping speed of 5 mm/min. The DPPE monolayer was dried in air for 30 min. To deposit the second layer, the DPPE monolayer in the trough was replaced with DPPC, DPPC/GM1 (90/10), or DPPC/cholesterol (2/1) with 2–10% GM1. The monolayers were compressed, annealed twice, and then transferred to DPPE-coated mica at a surface pressure of 45 mN/m. The resulting bilayers were kept under water in a preset small container and were kept under water during transfer to the AFM liquid cell (Molecular Imaging (MI), Phoenix, AZ).

### Bilayers from vesicle fusion

One milliliter of a chloroform solution of EPC or DPPC (1 mg/ml) with or without GM1 in a small vial was dried under a stream of nitrogen and then put under high vacuum overnight to form lipid films. The multilamellar vesicles were prepared by swelling the lipid films in phosphate-buffered saline solution (PBS buffer, 15 mM PO<sub>4</sub><sup>3-</sup>, 100 mM NaCl). The resulting multilamellar vesicles were then sonicated (Branson Instruments, Chicago, IL; D-50 bath-type sonicator) for 45 min at 45–50°C to obtain a clear solution of unilamellar vesicles (~50 nm in diameter), and 200  $\mu$ l of vesicle solution was used to form the bilayer on freshly cleaved mica clamped in the MI liquid cell. The incubation time (room temperature) was varied from 15 to 40 min to test for complete formation of an EPC bilayer on mica. For DPPC the mica was heated to 45°C during incubation. Before AFM imaging, the bilayers were rinsed extensively with PBS buffer.

### AFM measurements

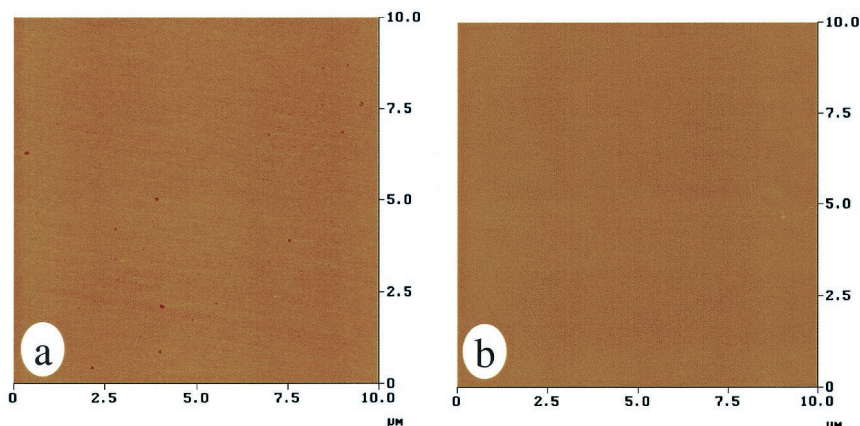
AFM measurements for monolayer samples were carried out on a multi-mode nanoscope III atomic force microscope (Digital Instruments, Santa Barbara, CA) in the repulsive mode in air. The J scanner (maximum scan area of 120  $\mu$ m  $\times$  120  $\mu$ m) and 200- $\mu$ m-long soft cantilevers with integrated pyramidal silicon nitride tips (spring constant of 60 mN/m) were used for all measurements. The scan force was ~2–4 nN, and the scan rate was typically 1 Hz. AFM measurements for bilayer samples were carried out on a Mac mode Picoscan atomic force microscope (Molecular Imaging) in the repulsive mode or in Mac mode (Han et al., 1996). The *x*-, *y*-, and *z*-scales were calibrated with a test pattern (3  $\mu$ m in *x*-scale and 26 nm for *z*-scale). In contact mode, silicon nitride tips with spring constants of ~60 mN/m were used. The force curves were obtained using the force spectroscopy feature of the MI machine. The imaging force was calibrated by recording a force curve on a hard surface (test pattern). The imaging force was minimized to 1 nN unless otherwise stated. Magnetic coated silicon tips with spring constants of 0.5 N/m and resonance frequencies between 25 and 40 kHz in aqueous solution were used for Mac mode measurements. The drive voltage was normally around 15 mV. Two different size scanners were used in the measurements with maximum scan areas of 30  $\times$  30  $\mu$ m<sup>2</sup> and 5  $\times$  5  $\mu$ m<sup>2</sup>. The scanning rate was 1 Hz. The bilayers prepared from Langmuir-Blodgett transfer were imaged in Milli-Q water. Before adding the cholera toxin B subunit, the aqueous solution was replaced with PBS buffer. Excess cholera toxin B subunit (10  $\mu$ g) was used to incubate with the bilayers for 30 min or longer. The bilayers were then rinsed extensively with buffer or water. Two or three independently prepared samples were imaged for each bilayer composition, and several areas were scanned for each sample. No attempt was made to account for tip-convolution effects for the smaller domains.

## RESULTS

### DPPC/DPPE bilayers

Hybrid bilayers with DPPC as the outer leaflet were deposited on DMPE-coated mica by Langmuir-Blodgett transfer. Images of initial monolayers of DPPC and DPPE deposited at 45 mN/m are shown in Fig. 1, *a* and *b*; both lipids yield uniform monolayers, although the DPPC monolayer has a significant number of pin-hole defects. A second DPPC layer can be deposited on both DPPC and DPPE monolayers. However, we find that more uniform bilayers with fewer defects are obtained using DPPE as the first layer. This is partially due to the lower number of defects in the original DPPE monolayer and a resulting lower probability

FIGURE 1 AFM images of DPPC (a) and DPPE (b) monolayers transferred to mica at 45 mN/m. The z-scale for both images is 5 nm.



of losing some of the bottom monolayer on the second transfer (Bassereau and Pincet, 1997). Similar results have also been reported previously (Rinia et al., 1999). Based on these results we have used a first layer of DPPE and a second layer of DPPC, both deposited at 45 mN/m, as our standard hybrid bilayer. Fig. 2 *a* shows a typical DPPC/DPPE bilayer with a smooth flat surface that is free of pin-hole defects but has several small areas of debris on the surface. To confirm that the smooth surface is in fact a bilayer, a small area of the same sample was scanned rapidly (15 Hz) with a much larger force (20 nN) for ~60 min before re-imaging a  $10 \times 10 \mu\text{m}^2$  area under standard conditions. The hole generated in the bilayer is clearly visible in Fig. 2 *b* and gives a thickness of ~5 nm (see inset of section analysis), consistent with deposition of a bilayer on the mica surface.

Incorporation of 10% GM1 in the top DPPC leaflet yields bilayers that are much less uniform than the DPPC/DPPE bilayer shown in Fig. 2 *a*. Fig. 2 *c* shows an example of a bilayer imaged immediately after deposition. The image shows a relatively uneven surface with small higher areas. Although the height difference is quite small, there is a somewhat more uniform, large domain in the center (~4  $\mu\text{m}$  in diameter), surrounded by a lower matrix that has a number of small dots that are ~2 nm in height. An identical sample that was stored overnight in water before imaging showed a bilayer with numerous small dots (Fig. 2 *d*, 100 nm in diameter and 2 nm in height) that were distributed randomly across the surface. The matrix in which the small dots are distributed is much more uniform than that for the fresh bilayer shown in Fig. 2 *c*. This sample was incubated with cholera toxin B subunit for 30 min and then rinsed with water and re-imaged (Fig. 2 *e*). The resulting bilayer shows numerous small dots that are ~200 nm in diameter but are much higher (12 nm) than those observed before protein addition, consistent with binding of protein to the small domains observed in the (GM1/DPPC)/DPPE bilayer alone. The fraction of the bilayer surface covered by the microdomains is ~10% for the image shown in Fig. 2 *d* and is

slightly larger (12–14%) after incubation with protein (Fig. 2 *e*). A control experiment in which a bilayer that did not contain GM1 was incubated with protein under identical conditions and then imaged did not provide any evidence for nonspecific adsorption of protein.

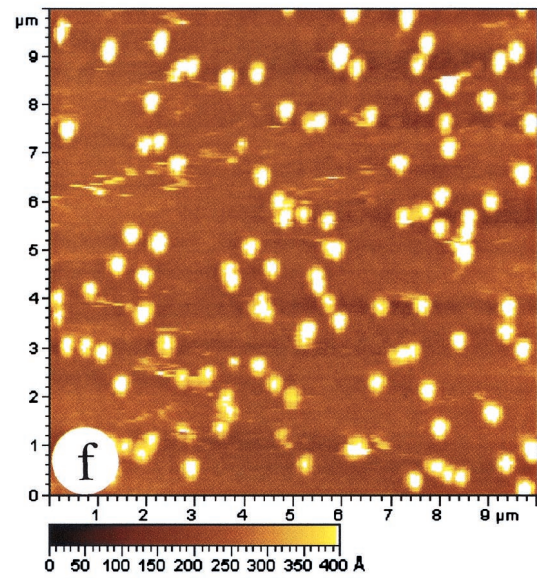
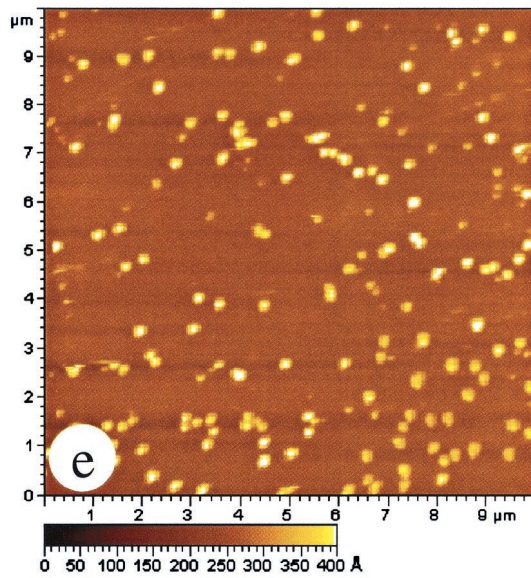
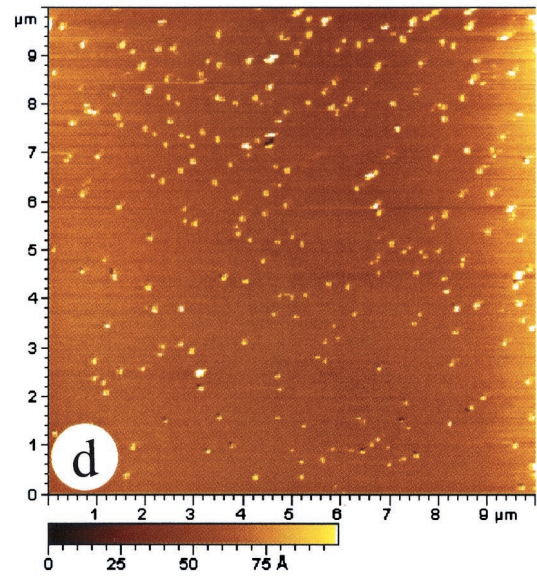
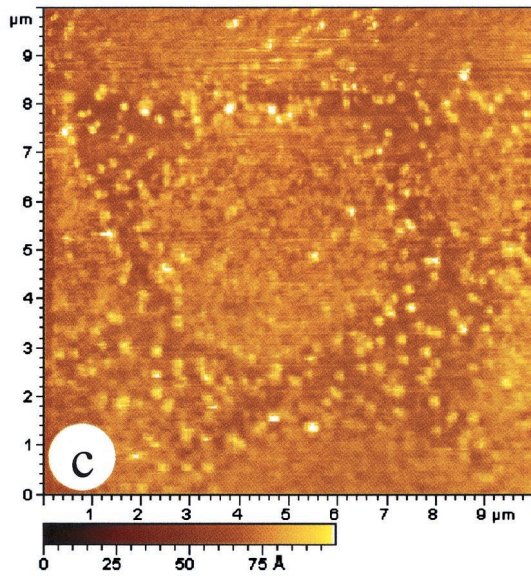
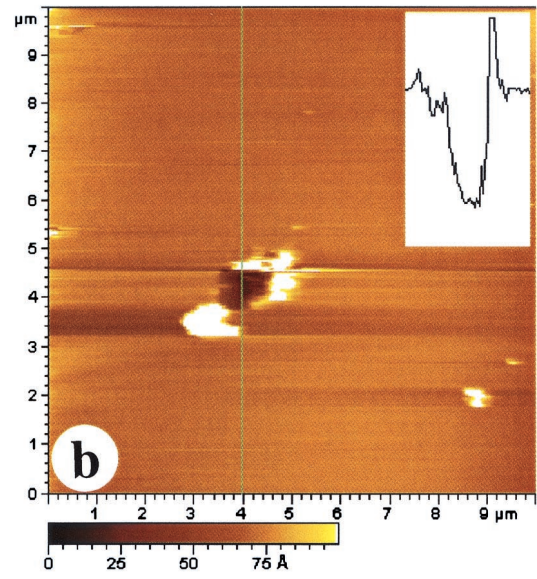
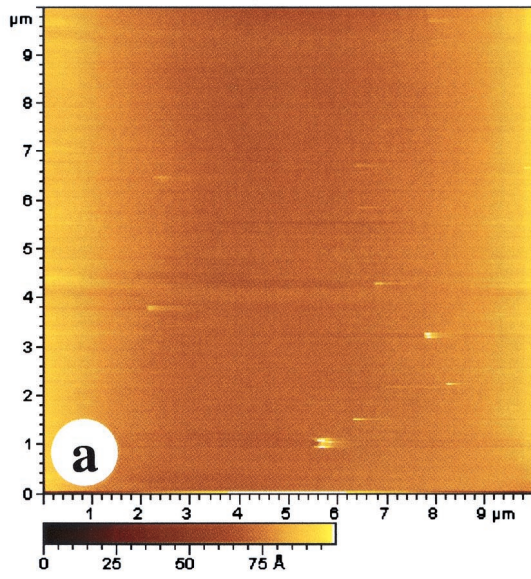
The above experiment for the (GM1/DPPC)/DPPE bilayer was repeated five times with similar results. In each case the bilayer showed very clear randomly scattered higher dots after a period of equilibration. Although the initial samples were less reproducible, they routinely showed significant heterogeneity when compared with a GM1-free bilayer. Furthermore, addition of protein resulted in selective binding to the small raised domains. The size of the domains was generally larger after protein addition and also increased slightly with longer incubation periods. This is clearly evident in comparing Fig. 2, *e* and *f*, which show bilayers after 30 and 90 min of incubation with protein; the diameter of the protein aggregates is ~50% larger for the longer incubation time. Consistent with this, the fraction of the surface covered by protein is ~20% after a longer incubation time.

Similar results were obtained for 5% GM1 in DPPC/DPPE bilayers in that GM1 addition always led to heterogeneous surfaces with small higher domains.

### (2:1 DPPC/cholesterol)/DPPE bilayers

Hybrid bilayers were also formed by depositing a 2:1 DPPC/cholesterol mixture (45 mN/m) on a DPPE monolayer. The 2:1 DPPC/cholesterol mixture was selected on the basis of our earlier monolayer results that had indicated that this mixture forms a uniform liquid-ordered phase (Yuan and Johnston, submitted for publication). The image in Fig. 3 *a* shows that the (DPPC/cholesterol)/DPPE bilayer also gives a uniformly flat surface with several small holes that are ~4.5 nm deep, consistent with bilayer deposition. Addition of GM1 to the top leaflet again results in heterogeneous samples as shown in Fig. 3, *b–d*, for 2%, 5%, and







10% GM1. Examination of a number of samples containing 2% and 5% GM1 indicates that the number of domains is similar for the two concentrations. However, the overall number of domains is significantly larger for samples containing 10% GM1. The size of the domains varies between  $\sim 30$  and 100 nm. Addition of cholera toxin B demonstrates that the protein localizes exclusively on the small higher domains, as shown in Fig. 3, *e* and *f*, for 5% and 10% GM1, respectively. The sample containing 5% GM1 shows protein domains that are  $\sim 150$  nm in diameter and 12 nm high. The domains are larger for the 10% GM1 sample (250–500 nm; 12 nm in height), and in several cases there are irregularly shaped domains formed by coalescence of two smaller ones. Several of the domains also have higher areas that are approximately twice the height and appear to result from an additional layer of protein (see section analysis in Fig. 3 *f*). There is no evidence of equilibration of the sample with time, as was observed for the DPPC/GM1 bilayers described above.

### EPC bilayers

Solutions of small unilamellar vesicles of EPC were incubated with mica for various time periods and then rinsed and imaged to find conditions for obtaining a uniform bilayer. Fig. 4 *a* shows a sample after incubation for 25 min; bilayer formation is incomplete, and there are areas of bare mica that are  $\sim 3$  nm below the lipid matrix, in agreement with previous measurements for similar bilayers (Reviakine and Brisson, 2000). Fig. 4 *b* shows an image of a complete bilayer formed after a 45-min incubation. This bilayer was incubated with cholera toxin for 30 min and then rinsed and re-imaged (Fig. 4 *c*); there is no evidence for binding of the protein to the EPC bilayer, indicating that nonspecific absorption of protein on the GM1-free bilayer does not occur. Fig. 4 *d* shows a similar bilayer prepared with 5% GM1/EPC. In this case there are small higher domains of variable size (50–100 nm) and height (2.5 nm, see inset of section analysis). After protein incubation for 30 min there are some much higher domains (Fig. 4 *e*, 6–7 nm), but there are still a significant number of domains that are similar in height to those observed before protein addition. Note that the conditions for protein incubation are similar to those used for other samples so the fact that protein adsorbs only on some of the domains is unlikely to result from insufficient time or amount of protein for complete coverage of GM1-rich areas.

### DPPC bilayers

DPPC bilayers were also prepared by vesicle fusion on mica for comparison with the results obtained for DPPC/DPPE bilayers prepared by Langmuir-Blodgett transfer. Proper choice of incubation conditions (45 min) and vesicle concentration again produced uniform bilayers with only occasional small defects or adsorbed debris. Addition of GM1 resulted in a heterogeneous bilayer with randomly distributed small domains (Fig. 4 *f*, 30–200 nm) that were again shown to adsorb protein (not shown).

### Effects of imaging force

The apparent height of the small domains observed in PC and PC/cholesterol bilayers changes significantly with the force applied in contact-mode AFM measurements. Fig. 5 shows AFM images for 10% GM1 in DPPC/DPPE and (2:1 DPPC/cholesterol)/DPPE bilayers recorded with two different imaging forces (note that these images are for the same samples shown in Figs. 2 *d* and 3 *d*). Fig. 5 *a* was recorded at an imaging force of 10 nN. The raised domains observed in Fig. 2 *d* at low imaging force now appear as holes. Decreasing the imaging force to 1 nN resulted in the reappearance of the higher domains with no apparent damage to the sample (Fig. 5 *c*). This indicates that the raised domains are part of the bilayer and are not due to debris on the bilayer surface. Interestingly, images recorded at intermediate forces show little evidence for either holes or raised domains in the bilayer (not shown). Section analysis shows that at the forces used to record the two images the holes and raised domains have apparent heights between 2 and 2.5 nm.

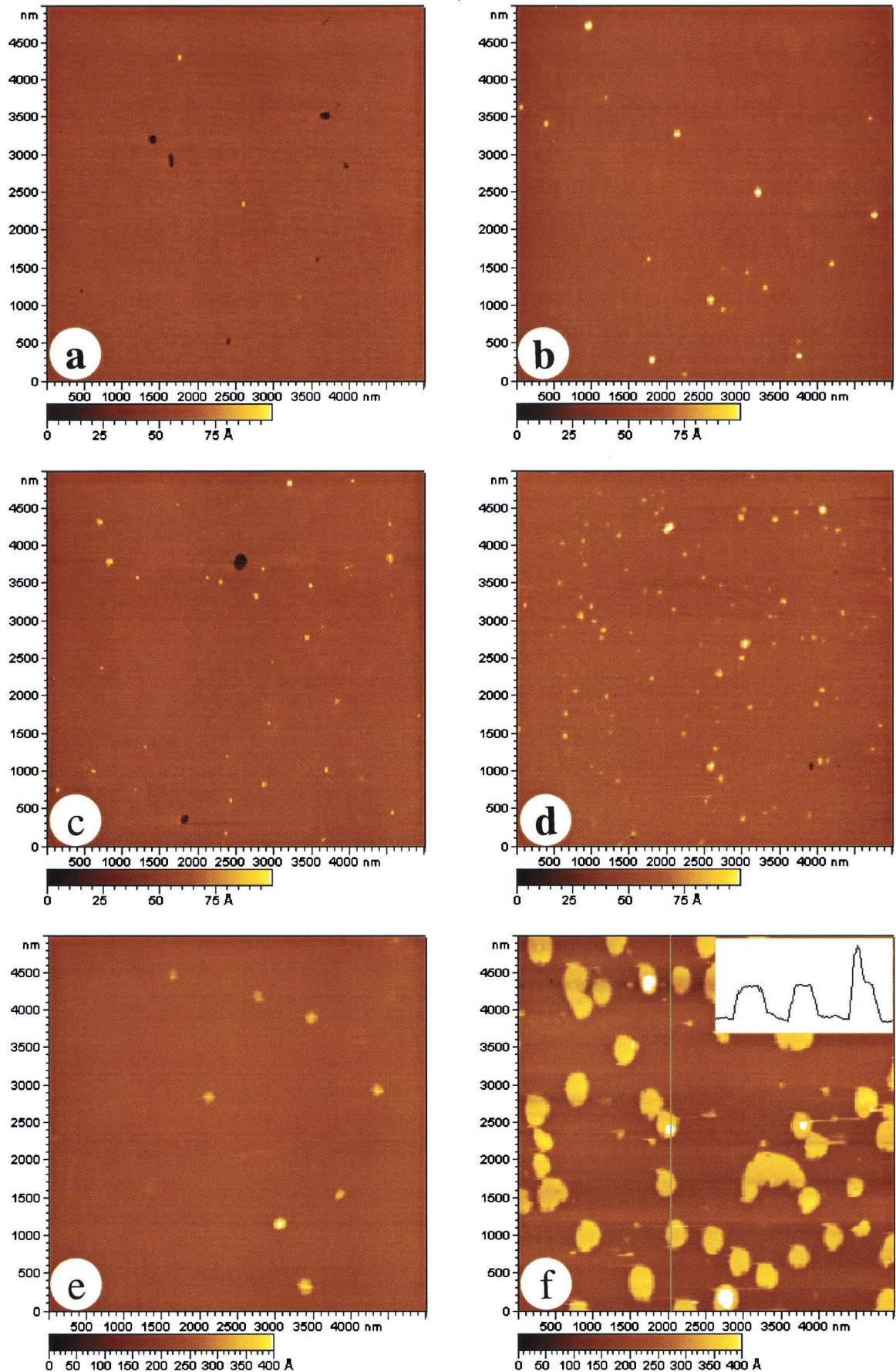
Similar results were also observed for samples containing 10% GM1 in a (2:1 DPPC/cholesterol)/DPPE bilayer, as shown in Fig. 5, *b* and *d*. The domains observed with an imaging force of  $\sim 1$  nN disappear completely at higher forces (Fig. 5 *b*). In this case the force ( $\sim 7$  nN) required to cause this image reversal is significantly lower than that needed to produce the same effect for the DPPC/DPPE bilayer. Decreasing the imaging force results in the reappearance of the raised domains (Fig. 5 *d*).

## DISCUSSION

Addition of GM1 to PC and PC/cholesterol bilayers results in heterogeneous samples that show numerous small do-

FIGURE 2 AFM images of hybrid DPPC/DPPE bilayers in the presence and absence of GM1 in the top DPPC layer. Both layers were transferred at 45 mN/m. (*a*) DPPC/DPPE bilayer. (*b*) Bilayer *a* after using an AFM tip to make a  $0.5\text{-}\mu\text{m}$  by  $0.5\text{-}\mu\text{m}$  hole in the bilayer. The inset section analysis shows a bilayer thickness of  $\sim 5$  nm (the *z*-scale for the section analysis is 10 nm). (*c*) (90/10 DPPC/GM1)/DPPE bilayer imaged immediately after transfer. (*d*) An identical bilayer to *c* imaged after equilibration overnight in water. (*e*) Bilayer *d* imaged after incubation with cholera toxin B subunit for 30 min and extensive rinsing with water. (*f*) A similar bilayer to *d* incubated with cholera toxin B subunit for 90 min.







mains varying in diameter from 30 to 200 nm. Both the fact that the domains appear only in the presence of GM1 and the increased length of the ganglioside as a result of the large oligosaccharide headgroup argue for localization of ganglioside in the small domains. Incubation of bilayers containing these GM1-rich domains with cholera toxin leads to specific binding of protein to the small domains with no evidence for its adsorption on other areas of the bilayer. This provides conclusive evidence for the localization of the ganglioside in the small raised domains. Similarly sized and shaped domains are observed in the various bilayers examined despite the considerable differences in fluidity of DPPC, EPC, and DPPC/cholesterol bilayers. The method of bilayer preparation also appears to have little effect on the overall morphology of the domains observed, although vesicle deposition does lead to domains in both upper and lower leaflets as discussed below.

There is evidence that equilibration of the initial GM1-doped bilayer occurs, at least for DPPC/DPPE bilayers made by Langmuir-Blodgett transfer. In fact, the observation of organization into large slightly higher domains surrounded by a heterogeneous lower phase is analogous to earlier results for DPPC monolayers deposited at high surface pressures (Yuan and Johnston, 2000). The GM1/DPPC monolayers also showed large domains that were heterogeneous on a sub-micron scale, which suggests that the initial bilayer retains the monolayer morphology. The observation of small round GM1-rich domains for various PC bilayers agrees well with results for 2–5% GM1 in cholesterol/DPPC monolayers that showed round islands for a range of surface deposition pressures. The monolayers at higher ganglioside loadings showed significant aggregation of the GM1-rich islands to give filamentous networks, unlike results in the bilayers. This indicates that aggregation of GM1 into small round domains represents a stable situation that is achievable under a variety of conditions in the more mobile supported bilayers. Although some of the phase separation behavior of transferred monolayers has been attributed to transfer artifacts (Shiku and Dunn, 1998; Vie et al., 1998), this does not appear to be an issue for using LB transfer to make supported bilayers. This is in agreement with recent observations of similar phase separation behavior for giant unilamellar vesicles and supported lipid bilayers (Dietrich et al., 2001) and is consistent with the greater mobility of supported bilayers versus monolayers (Boxer, 2000).

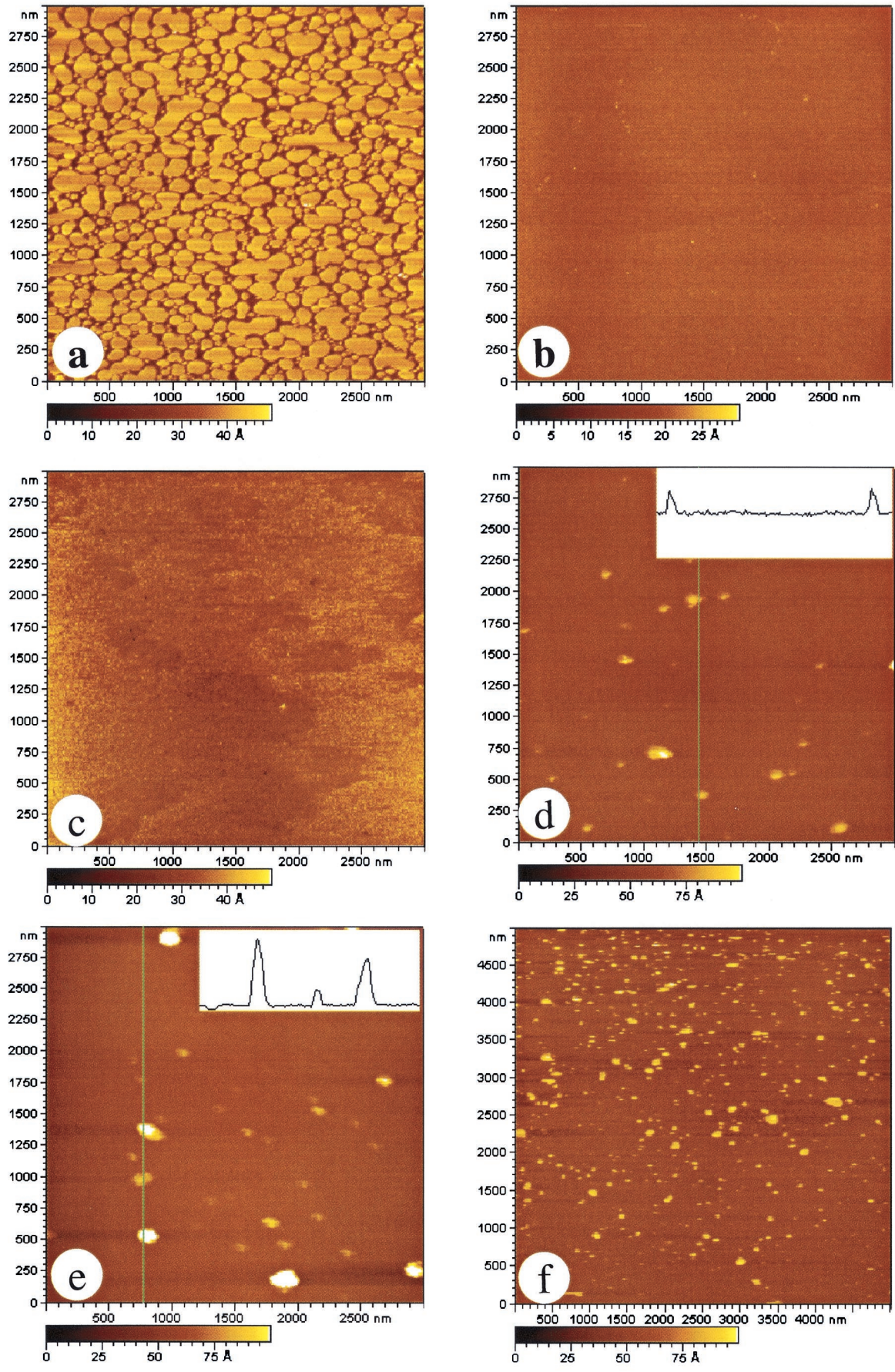
The images obtained upon incorporation of small amounts of GM1 in DPPC and DPPC/cholesterol bilayers

made by Langmuir-Blodgett transfer show no evidence for domains that do not bind protein. By contrast, only a fraction of the domains detected in EPC bilayers prepared by vesicle fusion were observed to bind protein. This indicates that there are GM1-rich domains in both the bottom and top leaflets, with only those domains in the top leaflet accessible for protein binding. This probably reflects the distribution of ganglioside in both the inner and outer monolayer of the initial vesicles, although the vesicle spreading/fusion process itself may also lead to an asymmetric distribution of GM1 in the final bilayer. It is also interesting to note that the domains are similar in size to the area that would be obtained from an individual vesicle (the estimated mean vesicle size of ~50 nm would result in a 100-nm-diameter bilayer disk). This suggests that there may be significant reorganization of the domains during bilayer formation by vesicle fusion. The AFM experiments do not provide any evidence for the existence of GM1-rich domains that span the bilayer, because these would be expected to be approximately twice the height of a single leaflet domain. This is in contrast to recent fluorescence experiments indicating that large micron-sized domains observed for giant unilamellar vesicles and supported bilayers span both leaflets of the bilayer (Bagatolli and Gratton, 2000; Dietrich et al., 2001; Korlach et al., 1999).

As noted above, the present results are in good agreement with monolayer results for similar lipid mixtures. However, they are in contrast to previous results in which AFM images had indicated complete coverage of several types of GM1-PC bilayers with cholera toxin (Mou et al., 1995) and with electron microscopy data that showed a random distribution of cholera toxin on GM1-doped bilayers (Thompson et al., 1985). Note that the earlier results had not provided any information on the distribution of ganglioside in the bilayers before protein incubation. It is clear that under our conditions the bilayer is heterogeneous, even before protein addition and under no conditions do we find complete or uniform coverage with protein. With longer incubation times we do find that the size of domains observed after protein addition is significantly larger. This may suggest that initial domains of GM1-adsorbed protein can induce adsorption of additional protein on the bilayer. Differences in the incubation conditions and sample preparation conditions may account for the fact that high and uniform coverage of the bilayer with cholera toxin was achieved in the previous work (Mou et al., 1995; Thompson et al., 1985).

FIGURE 3 AFM images of hybrid (2:1 DPPC/cholesterol)/DPPE bilayers in the presence and absence of GM1 in the top DPPC/cholesterol layer. (a) (2:1 DPPC/cholesterol)/DPPE bilayer. (b–d) (2:1 DPPC/cholesterol)/DPPE bilayers with 2% (b), 5% (c), and 10% (d) GM1 in the top layer. Images a–d were recorded immediately after transfer. (e and f) (2:1 DPPC/cholesterol)/DPPE bilayers with 5% GM1 (e) and 10% (f) GM1 in the top layer after incubation with cholera toxin B subunit for 30 min and rinsing with water. Image e was recorded immediately after rinsing with water, whereas image f was imaged after equilibration overnight in water. The inset section analysis ( $z$ -scale of 30 nm) for image f shows that the protein aggregates both laterally and vertically.







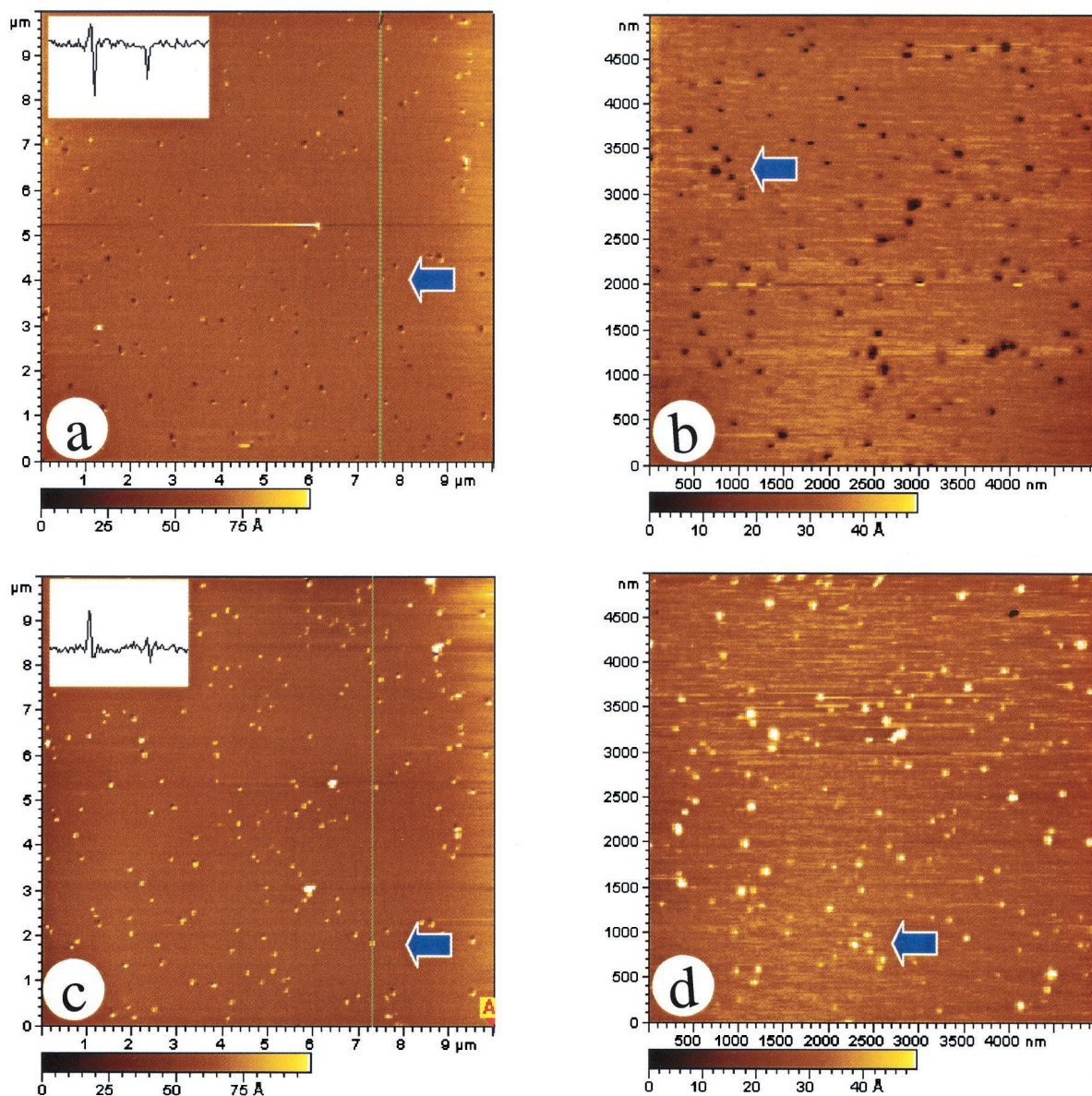


FIGURE 5 AFM images of hybrid bilayers of DPPC/DPPE and (2:1 DPPC/cholesterol)/DPPE with 10% GM1 in the outer DPPC layer imaged at different scanning forces. (a and c) DPPC/DPPE bilayer imaged at scanning forces of 10 nN and 1 nN, respectively. The arrow in each image was used to mark the same area as a reference and to denote the microdomain shown in the inset section analysis ( $z$ -scale of 5 nm). (b and d) (2:1 DPPC/cholesterol)/DPPE bilayer imaged at 7 nN and 1 nN, respectively.

The height that we measure for GM1 domains (2.5 nm at a scanning force of  $\sim 1$  nN) is higher than expected from x-ray diffraction data, which indicates that the GM1 molecule extends  $\sim 1.2$  nm beyond the bilayer surface (McIntosh

and Simon, 1994). This may be explained by the difference in interaction of the tip with the polar zwitterionic PC headgroups and the anionic oligosaccharide headgroups of the ganglioside. Electrostatic repulsion between the nega-

FIGURE 4 AFM images of egg PC and DPPC bilayers prepared by vesicle fusion. (a) Incomplete coverage for an egg PC bilayer obtained after 25 min incubation. (b) Complete coverage for an egg PC bilayer obtained with an incubation time of 45 min. (c) Bilayer b incubated with cholera toxin B subunit for 30 min and rinsed with water. (d) Egg PC bilayer with 5% GM1 prepared in the same way as bilayer b. The section analysis ( $z$ -scale 10 nm) shows that the GM1-rich domains are  $\sim 2.5$  nm higher than the bilayer. (e) Egg PC bilayer with 5% GM1 incubated with cholera toxin B subunit for 30 min and rinsed with water. The  $z$ -scale for the section analysis is 10 nm. (f) DPPC bilayer with 10% GM1 prepared by vesicle fusion.

tively charged silicon nitride tip and the polar GM1 head-group would be expected to result in a higher apparent height for the GM1 domains than for the surrounding neutral bilayer (Muller and Engel, 1997). The role of electrostatic effects has been well documented for a variety of biological samples and can lead to heights that vary by factors of 2–3, depending on the force applied and the imaging conditions (Muller and Engel, 1997). The importance of variations in tip-sample interactions as a function of sample composition is also evident when the imaging force is changed. The image reversal that is observed at high force is consistent with the tip penetrating the small domains at high loading and reflects the substantial difference in mechanical properties of the heterogeneous GM1-rich domains and the bulk PC phase. These results are analogous to the large changes in image contrast observed recently for phase-separated mixtures of saturated and unsaturated phosphatidylethanolamine bilayers (Dufrene et al., 1997; Schneider et al., 2000). Substantially less force is required to deform the raised domains in the DPPC/cholesterol bilayers.

The heights measured for protein aggregates formed by incubation of cholera toxin with the GM1-rich bilayers (Figs. 2 and 3) are higher than would be expected for a single layer of protein based on the crystal structure data for cholera toxin (Merritt et al., 1994). However, the uniformity of the protein aggregates and the fact that with lengthy incubation a second layer of protein appears for some domains both argue for a single protein layer. The heights measured using Mac mode for the EPC bilayers (Fig. 4) are considerably closer to the expected height for individual proteins bound to GM1-rich domains. This suggests that the apparent heights measured in contact mode reflect a combination of imaging force and electrostatic interactions, as outlined above for bilayers in the absence of protein.

The present results are of particular interest with respect to recent inconsistencies in the proposed sizes of lipid rafts. For example, fluorescence studies of PC/sphingomyelin/cholesterol monolayers demonstrate the localization of GM1 in sub-micron-sized domains of a condensed phase that is postulated to contain cholesterol/sphingomyelin complexes (Radhakrishnan et al., 2000). Similarly, confocal microscopy of supported lipid bilayers and giant unilamellar vesicles shows that GM1 is localized in large micron-sized domains for phase-separated bilayers with raft-like compositions (DOPC/sphingomyelin/cholesterol) (Dietrich et al., 2001). By contrast, much smaller rafts are proposed in natural membranes (Hwang et al., 1998; Jacobson and Dietrich, 1999; Pralle et al., 2000; Varma and Mayor, 1998). It has recently been hypothesized that the large domains observed for purified detergent-resistant membranes are formed by rearrangement of smaller microdomains during the extraction process (Giocondo et al., 2000). The AFM results described herein show that GM1 forms small sub-micron-sized domains in a variety of PC and PC/cholesterol bilayers. The small GM1 aggregates observed in PC bilayers

with a range of fluidities may not be readily detectable with the resolution available in the fluorescence microscopy experiments. This may provide an explanation for the apparent discrepancy in sizes for model membranes with raft-like compositions and those observed in natural membranes. In the latter case one may detect small aggregates of proteins that are localized in a larger liquid-ordered domain, similar to those detected by fluorescence in model lipid mixtures. AFM measurements for GM1 in PC/sphingomyelin/cholesterol mixtures confirm that small GM1-rich microdomains are also present in raft-like lipid mixtures (C. Yuan, J. Furlong, and L. J. Johnston, manuscript in preparation).

## REFERENCES

- Ahmed, S. N., D. A. Brown, and E. London. 1997. On the origin of sphingolipid/cholesterol-rich detergent insoluble cell membranes: physiological concentrations of cholesterol and sphingolipid induce formation of a detergent-insoluble, liquid-ordered lipid phase in model membranes. *Biochemistry*. 36:10944–10953.
- Bagatolli, L. A., and E. Gratton. 2000. Two-photon fluorescence microscopy of coexisting lipid domains in giant unilamellar vesicles of binary phospholipid mixtures. *Biophys. J.* 78:290–305.
- Bassereau, P., and F. Pincet. 1997. Quantitative analysis of holes in supported bilayers providing the adsorption energy of surfactants on solid substrate. *Langmuir*. 13:7003–7007.
- Boxer, S. G. 2000. Molecular transport and organization in supported lipid membranes. *Curr. Opin. Chem. Biol.* 4:704–709.
- Brown, D. A., and E. London. 1997. Structure of detergent-resistant membrane domains: does phase separation occur in biological membranes? *Biochem. Biophys. Res. Commun.* 240:1–7.
- Brown, D. A., and E. London. 1998. Functions of lipid rafts in biological membranes. *Annu. Rev. Cell Dev. Biol.* 14:111–136.
- Brown, D. A., and E. London. 2000. Structure and function of sphingolipid- and cholesterol-rich membrane rafts. *J. Biol. Chem.* 275:17221–17224.
- Brown, D. A., and J. K. Rose. 1992. Sorting of GPI-anchored proteins to glycolipid-enriched membrane subdomains during transport to apical cell surface. *Cell*. 68:533–544.
- Chi, L. F., M. Anders, H. Fuchs, R. R. Johnston, and H. Ringsdorf. 1993. Domain structures in Langmuir-Blodgett films investigated by atomic force microscopy. *Science*. 259:213–216.
- Delmelle, M., S. P. Dufrane, R. Brasseur, and J. M. Ruyschaert. 1980. Clustering of gangliosides in phospholipid bilayers. *FEBS Lett.* 121:11–14.
- Dietrich, C., L. A. Bagatolli, Z. N. Volovyk, N. L. Thompson, M. Levi, K. Jacobson, and E. Gratton. 2001. Lipid rafts reconstituted in model membranes. *Biophys. J.* 80:1417–1428.
- Dufrene, Y. F., W. R. Barger, J.-B. D. Green, and G. U. Lee. 1997. Nanometer-scale surface properties of mixed phospholipid monolayers and bilayers. *Langmuir*. 13:4779–4784.
- Giocondo, M.-C., V. Vie, E. Lesniewska, J.-P. Goudonnet, and C. Le Grimellec. 2000. In situ imaging of detergent resistant membranes by atomic force microscopy. *J. Struct. Biol.* 131:38–43.
- Han, W., S. M. Lindsay, and T. Jing. 1996. A magnetically driven oscillating probe microscope for operation in fluids. *Appl. Phys. Lett.* 69:4111–4114.
- Hwang, J., L. A. Gheber, L. Margolis, and M. Edidin. 1998. Domains in cell plasma membranes investigated by near-field scanning optical microscopy. *Biophys. J.* 74:2184–2190.
- Jacobson, K., and C. Dietrich. 1999. Looking at lipid rafts? *Trends Cell Biol.* 9:87–91.



- Korlach, J., P. Schwill, W. W. Webb, and G. W. Feigensohn. 1999. Characterization of lipid bilayer phases by confocal microscopy and fluorescence correlation spectroscopy. *Proc. Natl. Acad. Sci. U.S.A.* 96:8461–8466.
- McIntosh, T., and S. A. Simon. 1994. Long- and short-range interactions between phospholipid/ganglioside GM1 bilayers. *Biochemistry*. 33: 10477–10486.
- McKiernan, A. E., T. V. Ratto, and M. L. Longo. 2000. Domain growth, shapes and topology in cationic lipid bilayers on mica by fluorescence and atomic force microscopy. *Biophys. J.* 79:2605–2615.
- Merritt, E. A., S. Sarfaty, F. van den Akker, C. L'hoir, J. A. Martial, and W. G. J. Hol. 1994. Crystal structure of cholera toxin B-pentamer bound to receptor GM1 pentasaccharide. *Protein Sci.* 3:165–175.
- Mou, J., J. Yang, and Z. Shao. 1995. Atomic force microscopy of cholera toxin B-oligomers bound to bilayers of biologically relevant lipids. *J. Mol. Biol.* 248:507–512.
- Muller, D. J., and A. Engel. 1997. The height of biomolecules measured with the atomic force microscope depends on electrostatic interactions. *Biophys. J.* 73:1633–1644.
- Peters, M. W., and C. W. M. Grant. 1984. Freeze-etch study of an unmodified lectin interacting with its receptor in model membranes. *Biochim. Biophys. Acta.* 775:272–282.
- Peters, M. W., I. E. Mehlhorn, K. R. Baber, and C. W. M. Grant. 1984. Evidence of a distribution difference between two gangliosides in bilayer membranes. *Biochim. Biophys. Acta.* 778:419–428.
- Pralle, A., P. Keller, E.-L. Florin, K. Simons, and J. K. H. Horber. 2000. Sphingolipid-cholesterol rafts diffuse as small entities in the plasma membrane of mammalian cells. *J. Cell Biol.* 148:997–1007.
- Radhakrishnan, A., T. G. Anderson, and H. M. McConnell. 2000. Condensed complexes, rafts and the chemical activity of cholesterol in membranes. *Proc. Natl. Acad. Sci. U.S.A.* 97:12422–12427.
- Reviakine, I., and A. Brisson. 2000. Formation of supported phospholipid bilayers from unilamellar vesicles investigated by atomic force microscopy. *Langmuir*. 16:1806–1815.
- Reviakine, I., A. Simon, and A. Brisson. 2000. Effect of  $\text{Ca}^{2+}$  on the morphology of mixed DPPC-DOPS supported phospholipid bilayers. *Langmuir*. 16:1473–1477.
- Rinia, H. A., R. A. Demel, J. P. J. M. van der Eerden, and B. de Kruijff. 1999. Blistering of Langmuir-Blodgett bilayers containing anionic phospholipids as observed by atomic force microscopy. *Biophys. J.* 77: 1683–1693.
- Sackmann, E. 1996. Supported membranes: scientific and practical applications. *Science*. 271:43–48.
- Schneider, J., Y. F. Dufrene, W. R. Burger, and G. U. Lee. 2000. Atomic force microscope image contrast mechanisms on supported lipid bilayers. *Biophys. J.* 79:1107–1118.
- Schroeder, F., J. K. Woodford, J. Kavecansky, W. G. Wood, and C. Joiner. 1995. Cholesterol domains in biological membranes. *Mol. Membr. Biol.* 12:113–119.
- Shiku, H., and R. C. Dunn. 1998. Direct observation of DPPC phase domain motion on mica surfaces under conditions of high relative humidity. *J. Phys. Chem.* 102:3791–3797.
- Simons, K., and E. Ikonen. 1997. Functional rafts in cell membranes. *Nature*. 387:569–572.
- Simons, K., and E. Ikonen. 2000. How cells handle cholesterol. *Science*. 290:1721–1726.
- Sparr, E., K. Ekelund, J. Engblom, S. Engstrom, and H. Wennerstrom. 1999. An AFM study of lipid monolayers. II. Effect of cholesterol on fatty acids. *Langmuir*. 15:6950–6955.
- Thompson, T. E., M. Allietta, R. E. Brown, M. L. Johnston, and T. W. Tillack. 1985. Organization of ganglioside GM1 in phosphatidylcholine bilayers. *Biochim. Biophys. Acta.* 817:229–237.
- Varma, R., and S. Mayor. 1998. GPI-anchored proteins are organized in submicron domains at the cell surface. *Nature*. 394:798–801.
- Vie, V., N. V. Mau, E. Lesniewska, J. P. Goudonnet, F. Heitz, and C. L. Grimellec. 1998. Distribution of ganglioside GM1 between two-component, two-phase phosphatidylcholine monolayers. *Langmuir*. 14: 4574–4583.
- Yuan, C., and L. J. Johnston. 2000. Distribution of ganglioside GM1 in L- $\alpha$ -dipalmitoylphosphatidylcholine/cholesterol monolayers: a model for lipid rafts. *Biophys. J.* 79:2768–2781.